



# Materials Science

An Indian Journal

Full Paper

MSAIJ, 10(6), 2014 [225-231]

## Behaviour at high temperature of two cobalt-based superalloys reinforced by carbides. Part 1: Case of a high carbon {Co-1C-21.5Cr-4.5Ta-9W}-based superalloy

Pierre-Yves Girardin<sup>1</sup>, Adrien Frigerio<sup>1</sup>, Patrice Berthod<sup>2\*</sup>

<sup>1</sup>Lycée Henri Loritz, 29 Rue des Jardiniers 54000 Nancy, (FRANCE)

<sup>2</sup>Institut Jean Lamour (UMR CNRS 7198), department CP2S, team "Surface and Interface, Chemical Reactivity of Materials", University of Lorraine, B.P. 70239, 54506 Vandoeuvre-lès-Nancy, (FRANCE)

E-mail : patrice.berthod@univ-lorraine.fr

### ABSTRACT

After having presented the as-cast microstructures of two complex carbide-strengthened cast cobalt-based alloys replicated with a fine microstructure in laboratory by melting of pure elements, this work, presented in two parts, aims specifying the high temperature oxidation and high temperature microstructural behaviours at two levels of temperature - 1050°C and 1150°C – and for two durations - 66 hours and 146 hours – of these two alloys. In this first part it the case of the Co(bal.)-1C-21.5Cr-4.5Ta-9W (wt.%) which is under consideration. It appeared here that this alloy did not behave very well in oxidation, already at 1050°C but especially at 1150°C, temperature at which catastrophic oxidation occurred early. At the lowest tested temperature the carbide population did not significantly evolve while a more important difference appeared at 1150°C: the loss of the chromium-tungsten carbides. The latter phenomenon induced a decrease in room temperature hardness.

© 2014 Trade Science Inc. - INDIA

### KEYWORDS

Commercial Co-based superalloy;  
High temperature microstructure;  
Hot oxidation;  
Room temperature hardness.

### INTRODUCTION

Among the numerous superalloys existing for meeting high temperature applications' needs there are the cast cobalt-based ones which present for many of them the double particularity to resist hot corrosion by containing rather high quantities of chromium<sup>[1]</sup>, and high temperature mechanical solicitations – creep deformation notably – by the presence of interdendritic primary carbides (and also often of secondary fine carbides precipitated in the matrix)<sup>[2]</sup>. This is for instance the case of the two well-known commercial Co-based superalloys

MarM-322 and MarM-509<sup>[3]</sup>. As recently seen<sup>[4]</sup>, when their conditions of elaboration (by casting) are favourable to a fast cooling (small ingot, water-cooled metallic mould) then to a rather fast solidification, their microstructures contain again primary carbides, of two types (chromium carbides and MC carbides), allowing them to potentially benefit of these strengthening particles in the high temperature mechanical field. This is really true only if these carbides do not evolve too rapidly when the superalloy is working at high temperature.

In this study the two cobalt-based superalloys, the as-cast microstructures and room temperature hard-

## Full Paper

ness of which were studied in a recent work<sup>[4]</sup>, were subjected to more or less long exposures at two high temperatures in oxidizing atmospheres, in order to observe how they behave in hot oxidation and also to see how their microstructures are changing with time at high temperature. In this first part the case of the laboratory alloy CoX representing the commercial MarM-322 with a finer microstructure is examined.

### EXPERIMENTAL

#### The alloy under study

One can remind first that the alloy CoX elaborated in laboratory by targeting the chemical composition of the MarM-322, Co(bal.)-21.5Cr-1C-4.5Ta-0.75Ti-9W-0.5Fe-2Zr, was in fact obtained with the following composition\*: Co(bal.)-22.31Cr-1\*\*C-4.92Ta-0.66Ti-10.65W-0.73Fe-1.50Zr (\*: technique used: Energy Dispersion Spectrometry; \*\*: cannot be measured because too light element, content supposed to be respected). Second, its as-cast microstructure is composed of a cobalt matrix containing essentially Cr and W in solid solution, blocky chromium carbides rich in Cr but also in W, and two types of MC carbides (rich in Ta and Zr, and also Ti): some of them compact and the other - script-like - obviously forming an eutectic with the matrix. This microstructure is illustrated by the micrograph given in Figure 0 (left side) and it can be commented by the graph given in the same Figure

(right side), plotted with the results of thermodynamic calculations performed using the Thermo-Calc software<sup>[5]</sup> and a database issued from the SSOL one<sup>[6]</sup>. This database, which already contained the descriptions of the Co-Cr-C systems and its sub-systems<sup>[7-12]</sup>, was enriched with additional systems' descriptions<sup>[13-15]</sup> concerning the presence of Ta (for a correct prevision of the TaC-based carbides). On this graph it can be seen that solidification effectively starts, not by the crystallization of the matrix but by the MC carbides (probably the blocky ones). When temperature reaches the eutectic reaction temperature range, a second part of MC carbides precipitates together with matrix, this leading to the eutectic MC carbides. At the same time  $M_7C_3$  carbides would start appearing and grow during a first part of solid state cooling over about 200°C. For lower temperatures they would transform into  $M_{23}C_6$  carbides, a part of which, at temperatures near 1000°C may transform into other carbides. As one saw above, such chromium carbides were effectively encountered in the as-cast microstructure.

#### The high temperature tests

The same ingot as the one cut to obtain the metallographic sample for the characterization of the as-cast microstructure was also used to obtain, by cutting, four samples for the high temperature exposures. Samples of about 100mm<sup>3</sup> were obtained and one of their two main faces was polished with 1200-grit SiC paper. They

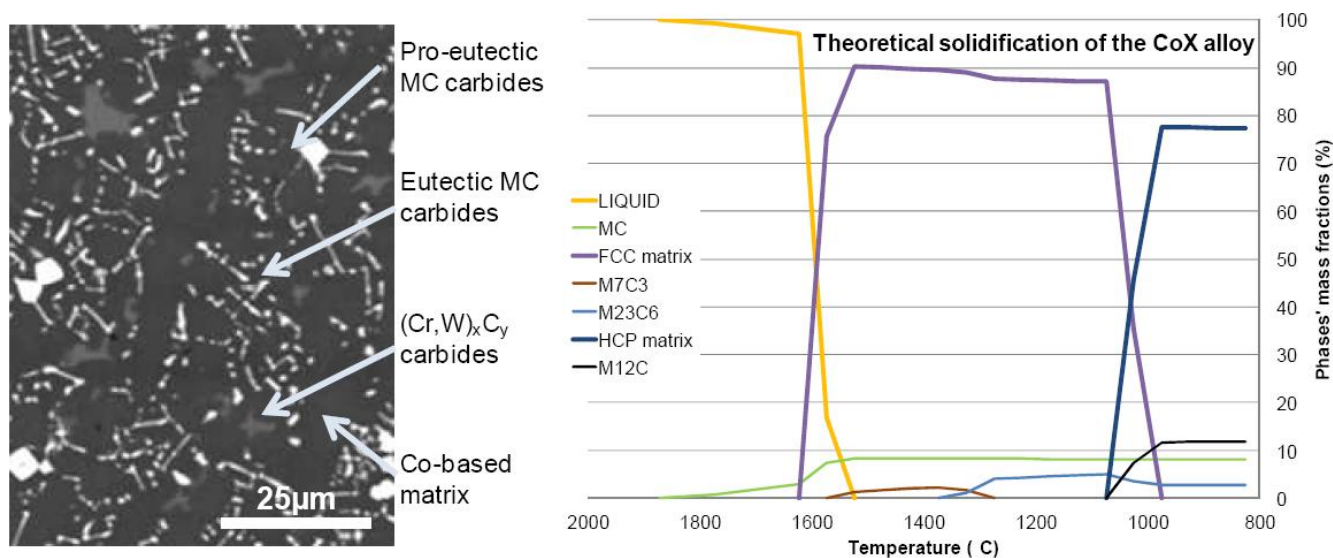


Figure 0 : Micrograph (Scanning Electron Microscope in Back Scattered Electrons mode) of the as-cast microstructure of the CoX alloy (left side) and theoretic solidification sequences plotted from Thermo-Calc calculations' results (on the right)

were put in an alumina nacelle which was placed inside a resistive tubular furnace Carbolite. The heating was realized at  $10^{\circ}\text{C min}^{-1}$  from room temperature up to one of the two targeted temperatures ( $1050^{\circ}\text{C}$  and  $1150^{\circ}\text{C}$ ). The dwell durations were 66 hours and 146 hours for the two temperatures. These four oxidation tests in laboratory air were finished by a slow cooling in furnace after shutting off. Just after return to room temperature and before the following preparation steps, the oxidized samples were weighed again and the mass difference calculated.

### Metallographic preparation and observations

The oxidized samples were first subjected to gold deposition by cathodic pulverization (to allow the external border of the oxide to be electrically conductive for the subsequent operation), covered by a sufficiently thick layer of electrolytic nickel (deposited by reduction of the  $\text{Ni}^{2+}$  anions of a Watt's bath heated to  $50^{\circ}\text{C}$ ), cut and embedded in a cold resin mixture (ESCIL: Araldite CY230 and hardener HY 956) to obtain cross sections to observe and analyze. The obtained embedded samples were then polished with SiC papers with grade from 120 or 240 up to 1200, under water. Thereafter they were ultrasonically cleaned then subjected to a final polishing phase with a textile disk enriched in  $1\mu\text{m}$  hard particles, in order to obtain a mirror-like surface state.

Bulk, sub-surface and external oxides were all observed using a JEOL JSM 6010LA Scanning Electron Microscope (SEM). These examinations were essentially done in Back Scattered Electrons (BSE) mode at different magnifications, between  $\times 250$  and  $\times 1000$  principally. The Energy Dispersive Spectrometry (EDS) device equipping the SEM was used to specify the different types of oxides present either externally in the scales formed over the alloys, or internal ones appeared in the subsurface. The same technique and apparatus were used to perform pinpoint measurements to obtain concentration profiles from the {external oxide}-alloy interface.

To finish, for each of the four samples exposed to high temperature, three micrographs taken in BSE mode in the bulk were analyzed using the image analysis tool of the Photoshop CS software of Adobe, to obtain the surface fractions of the different types of carbides.

### Macro-hardness measurements

Vickers indentations were performed on these new mounted samples, for comparison with the results obtained for the as-cast alloy. Here too this was done by applying a load of 30 kg with a Testwell Wolpert machine. Similarly three indentations were realized and the three values of hardness were used to calculate the average hardness and a value of standard deviation.

## RESULTS AND DISCUSSION

### General aspect of the alloys after oxidation tests

The surfaces states of the alloys after exposure for 66h or 146h at  $1050^{\circ}\text{C}$  or  $1150^{\circ}\text{C}$  are illustrated in Figure 1 with one (or two when both sides were scanned) pictures per sample. One can globally see that the CoX alloy was logically more oxidized for a higher temperature for a same duration and for a longer duration for a given temperature. The external oxide scales were lost during cooling in most cases, even for the rather low cooling rate applied (in shut off furnace). The oxidation appears having been severe at  $1150^{\circ}\text{C}$ , notably when the duration was the longest (146h). For this last sample one can notice a particularly strong oxidation of the edges and corners.

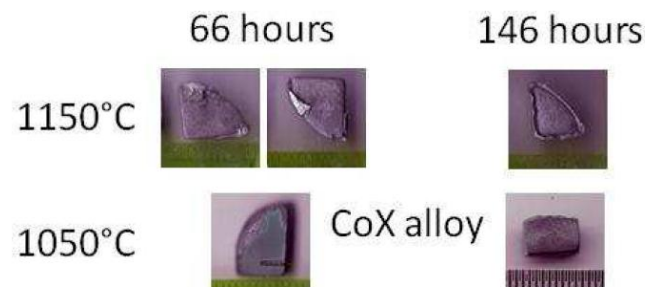


Figure 1 : Scanned images of the oxidized samples (scanned)

### Surfaces and sub-surfaces: characteristics of the oxides formed and chemical modifications in the alloy

The surface and subsurface states of three of the four oxidized samples are illustrated in Figure 2 (CoX alloy after 66h at  $1050^{\circ}\text{C}$ ), Figure 3 (after 146h at  $1050^{\circ}\text{C}$ ) and Figure 4 (after 66h at  $1150^{\circ}\text{C}$ ).

The sample oxidized at  $1050^{\circ}\text{C}$  during 66h (Figure 2) presents a rather irregular surface which is however covered by chromia ( $\text{Cr}_2\text{O}_3$ ). From this surface

Full Paper

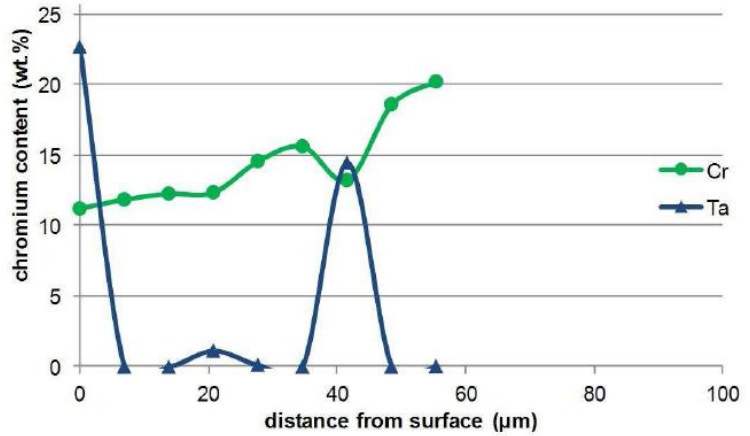
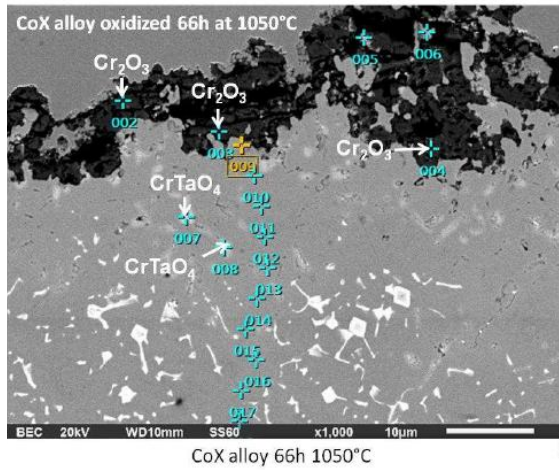


Figure 2 : Micrograph of the surface and subsurface of the CoX alloy oxidized during 66h at 1050°C, with identification of the different oxides and the concentration profile (of the Cr and Ta only) acquired on the points marked on the micrograph

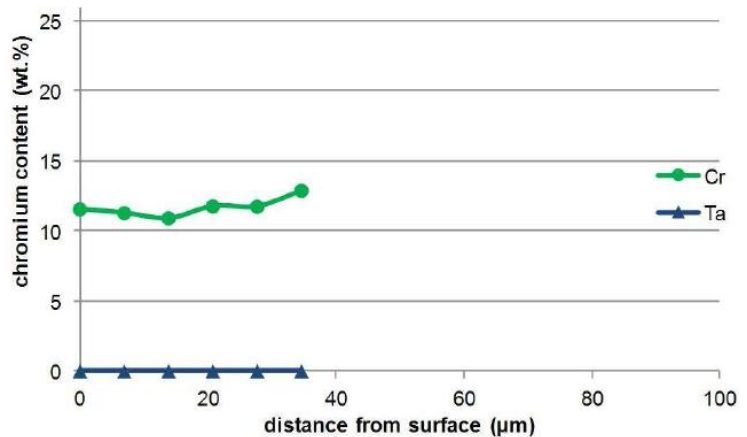
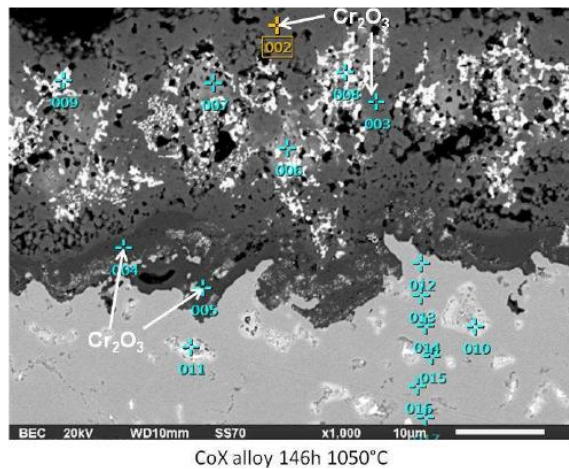


Figure 3 : Micrograph of the surface and subsurface of the CoX alloy oxidized during 146h at 1050°C, with identification of the different oxides and the concentration profile (of the Cr and Ta only) acquired on the points marked on the micrograph

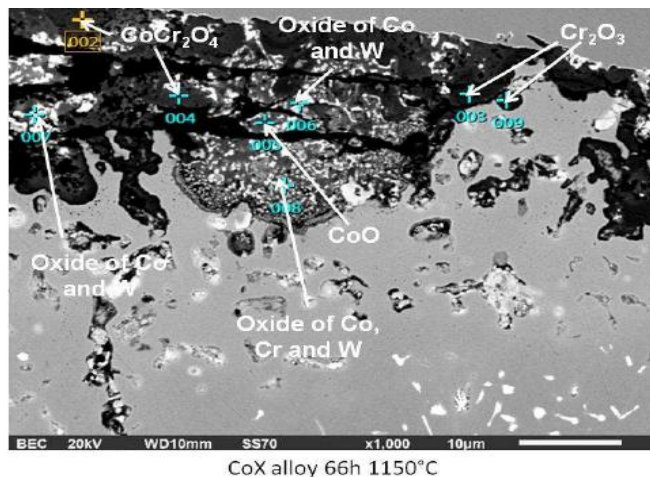


Figure 4 : Micrograph of the surface and subsurface of the CoX alloy oxidized during 66h at 1150°C, with identification of the different oxides

the carbides have disappeared over a depth of about 10-15 µm while CrTaO<sub>4</sub> internal oxides have appeared inside this carbide-free zone. EDS concentration profiles have been acquired and are presented for the Cr and Ta elements only. From the oxide/alloy interface the chromium content increases from about 12 wt.% to 20 wt.% over about 60 µm while the tantalum content stays almost zero except when the pinpoint measurement is down on a MC carbide. From several profiles performed as the one above it appeared that the chromium content in extreme surface varies in fact between 10.4 and 12.2wt.%.

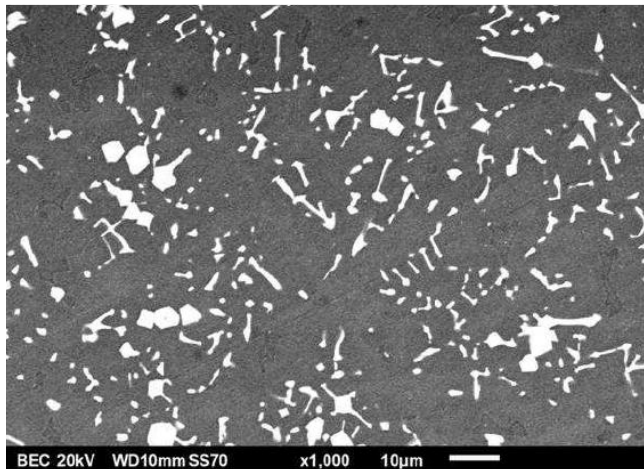
The sample oxidized at the same temperature but during 146 hours (Figure 3) is covered by a much thicker oxide scale, which is composed of several types of ox-

ides:  $\text{Cr}_2\text{O}_3$  but also complex oxides some of them involving the heaviest atoms present in the alloy. The EDS profiles of Cr and Ta concentrations also show chromium contents in extreme surface decreased down to values comprised between 10.3 and 11.5wt.%, with however some rare locations in which values as 17.5wt.%Cr were obtained.

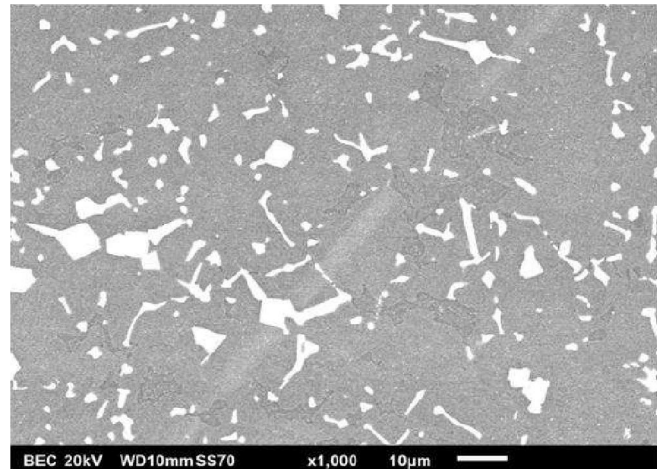
Catastrophic oxidation also affected the samples oxidized at  $1150^\circ\text{C}$  during 66 hours (Figure 4) and the one oxidized at this same higher temperature but during 146 hours. Indeed, thick multi-constituted oxides are present and the chromium contents in extreme surface are very low, between 2.7 and 5.1 wt.% ( $1050^\circ\text{C}$ ) and 4.6 to 6.4 wt.% ( $1150^\circ\text{C}$ ).

### Bulk microstructures after high temperature exposures; new values of hardness

During exposures as temperatures higher than  $1000^\circ\text{C}$  and during several tens hours, there is not only the subsurface which may be affected as this was observed above (development of carbide-free zone, internal oxidation, chromium depletion and also diffusion of other elements), but also the bulk microstructures may have evolved. If no real change can be seen in the bulk of the CoX samples after exposure to  $1050^\circ\text{C}$  for 66 or 146 hours (Figure 5), it seems, in contrast, that a great difference in its bulk microstructure appeared after exposure to  $1150^\circ\text{C}$ , whatever the duration: the

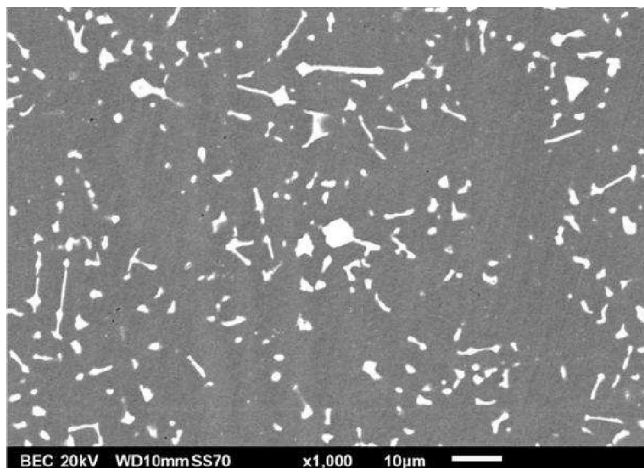


CoX alloy after 66h  $1050^\circ\text{C}$

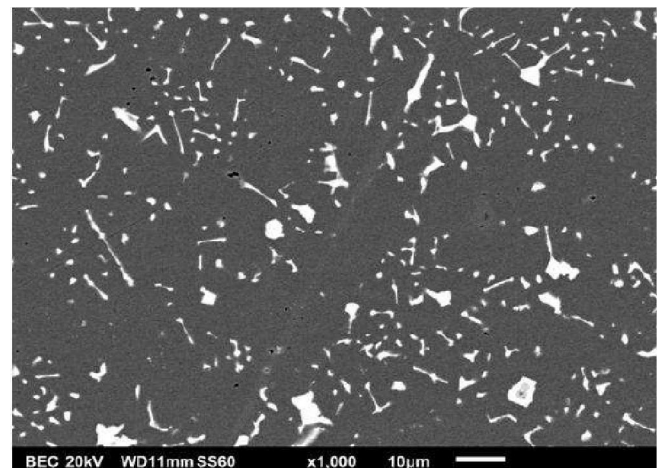


CoX alloy after 146h  $1050^\circ\text{C}$

**Figure 5 :** Micrographs illustrating the bulk microstructure of the studied CoX alloy after exposure at  $1050^\circ\text{C}$  during 66h (left) and during 146h (right); white MC carbides and darker carbides of chromium and tungsten



CoX alloy 66h  $1150^\circ\text{C}$



CoX alloy 146h  $1150^\circ\text{C}$

**Figure 6 :** Micrographs illustrating the bulk microstructure of the studied CoX alloy after exposure at  $1150^\circ\text{C}$  during 66h (left) and during 146h (right); only white MC carbides

## Full Paper

obvious disappearance of the chromium carbides (Figure 6).

The surface/volume fractions of the carbides as measured using Adobe Photoshop are graphically given in Figure 7. These measurements concern only the MC carbides, the white colour of which greatly

facilitates image analysis. The colour of the chromium carbides being too close to the matrix one it was

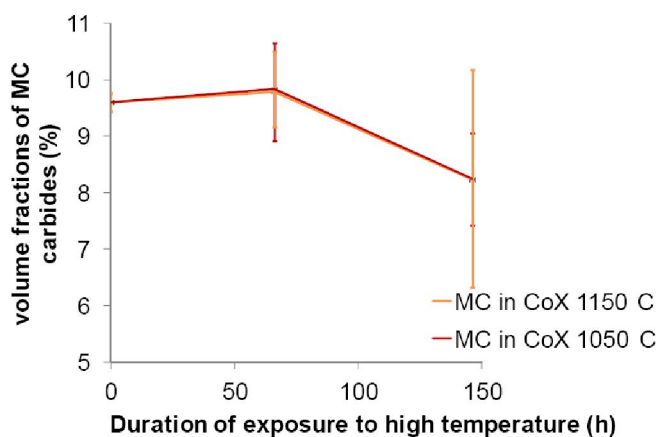


**Figure 7 : Evolution of the carbide fractions (MC-carbides only) of the CoX alloy with time for the two temperatures**

not possible to determine their surface fractions with accuracy. One can see that the surface fractions of the MC-carbides do not really depend on temperature but on exposure time since they significantly decrease between 66 hours and 146 hours (they loss about 2 surf.% or vol.%).

Hardness measurements were done on the samples with their four aged states. The results are graphically presented in Figure 8. One can see on this graph that the hardness remains almost independent on the aging duration at 1050°C (no significant differences between as-cast, 66h and 146h by considering the error bars) while, in contrast, hardness falls with the first hours of aging at 1150°C since the hardness after 66h and after 146h at this temperature are 50Hv lower than in the as-cast condition.

### General commentaries

Thus, the CoX alloy correctly behaved in oxidation at high temperature only at 1050°C and this over a duration comprised between 66 hours and 146 hours. During the 66 first hours at this temperature chromia nucleated and grew on the sample surface until forming a continuous protective of this almost stoichiometric ox-

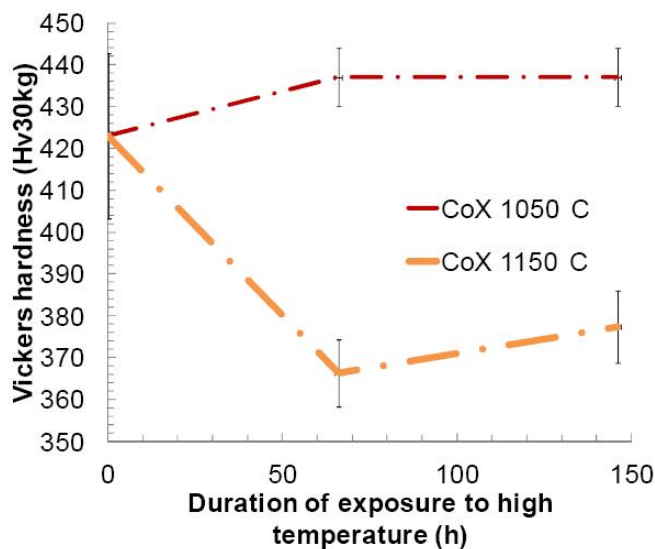


**Figure 8 : Evolution of the hardness of the CoX alloy with the temperature and the duration of the exposure to high temperature**

ide. This induced an impoverishment in this element of the sub-surface, with as result a depleted zone extended deeper than the carbide-free zone. The low level of chromium concentration near the alloy surface (only 12 wt.%Cr) allowed anticipating the loss of this chromia-forming behaviour as observed at 146 hours. This chromia-forming behaviour loss was logically much sooner for the sample exposed to 1150°C. This demonstrates that this fine microstructure alloy, in absence of any coating of protection against oxidation, cannot be used at so elevated temperature.

The exposure to high temperature had also consequences for the bulk microstructure of the alloy but this is particularly true for 1150°C since the chromium-tungsten carbides have obviously disappeared (while the MC carbides seem having remained unchanged) This was confirmed by the significant decrease in hardness observed for the bulk of the samples oxidized at 1150°C for 66h and 146h, that the disappearance of the chromium carbides easily explains.

### CONCLUSIONS

This finely micro-structured version of the MarM-322 commercial alloy, with - it is true - some small discards for the contents in several elements, is obviously not greatly resistant against high temperature oxidation. Oxidation threatens becoming catastrophic after about

a hundred hours at 1050°C, what occurs already after only several tens of hours at 1150°C. This may be due to the rather low chromium content of this alloy (only 21.5 wt.%Cr). Furthermore the mechanical properties may be weakened at 1150°C with the loss of one of the two main types of carbides: the carbides of chromium and tungsten. In the second part of this work we will examine if the finely micro-structured version of the MarM-509 alloy presents better properties in high temperature oxidation (a little richer in chromium) and in sustainable mechanical resistance.

### REFERENCES

- [1] P.Kofstad; High Temperature Corrosion, Elsevier applied science, London, (1988).
- [2] C.T.Sims, W.J.Hagel; The Superalloys, John Wiley and Sons, New York, (1972).
- [3] E.F.Bradley; Superalloys: A Technical Guide, 1<sup>st</sup> Edition, ASM International, Metals Park, (1988).
- [4] A.Frigerio, P.Y.Girardin, P.Berthod; Materials Science: An Indian Journal, accepted paper.
- [5] Thermo-Calc version N: Foundation for Computational Thermodynamics, Stockholm, Sweden, Copyright, (1993,2000).
- [6] SGTE: Scientific Group Thermodata Europe database, update, (1992).
- [7] A.Fernandez Guillermet; Int.J.Thermophys., **8**, 481 (1987).
- [8] J.O.Andersson; Int.J.Thermophys., **6**, 411 (1985).
- [9] P.Gustafson; Carbon, **24**, 169 (1986).
- [10] A.Fernandez Guillermet; Z.Metallkde, **78**, 700 (1987).
- [11] J.O.Andersson; Calphad, **11**, 271 (1987).
- [12] A.Fernandez Guillermet; Z.Metallkde., **79**, 317 (1988).
- [13] K.Frisk, A.Fernandez Guillermet; J.Alloys Compounds, **238**, 167 (1996).
- [14] Z.K. Liu, Y.Austin Chang; Calphad, **23**, 339 (1999).
- [15] N.Dupin, I.Ansara; J.Phase Equilibria, **14**, 451 (1993).